JOURNAL OF SPACECRAFT AND ROCKETS
Vol. 44, No. 6, November–December 2007

Mars Thermospheric Winds from Mars Global Surveyor and Mars Odyssey Accelerometers

Geoff Crowley*
Atmospheric & Space Technology Research Associates, San Antonio, Texas 78249
and
Robert H. Tolson†
North Carolina State University, Raleigh, North Carolina 27695

DOI: 10.2514/1.28625

There have been no Mars thermospheric wind measurements, and so our knowledge of thermospheric winds comes from model predictions. Wind measurements are important for both fundamental and applied scientific research. Previously, Mars Global Surveyor and Odyssey in-track accelerometer data have been used to derive atmospheric densities during aerobraking. We describe initial results from a new technique to derive cross-track winds from spacecraft accelerometer and rate gyro data in the 95–160-km region. Preliminary estimates of densities and winds are presented for 10 orbits while Odyssey is sampling the winter polar vortex during November 2001–January 2002 ($L_s = 267$–290). The data are placed in context using a new general circulation model: the advanced space environment model. The model is a first-principles fully coupled, three-dimensional, general circulation model that extends from 14-km altitudes to the upper thermosphere near 250 km. It solves for the neutral winds, neutral temperature, electron and ion temperature profiles, and electron density, as well as for the major neutral species, many minor species, and appropriate ion chemistry. Comparison of the Odyssey cross-track winds with winds from the new model confirms that the initial wind results from our technique are reasonable. Both the data and the model suggest that large wind shears are present in the lower thermosphere.

I. Introduction

KNOWLEDGE of winds is important for spacecraft engineering and safety. Wind measurements are important for improvement of atmospheric models that further the understanding and forecasting of Mars atmospheric conditions affecting aerobraking. Wind measurements are needed to validate the model predictions and help to improve the models for use in planning future missions. Neutral winds in the upper atmosphere of Mars are of fundamental scientific concern, because they provide insight into the energetics and dynamics of the planetary atmosphere. The winds are driven primarily by pressure gradients caused by solar heating of the upper atmosphere. They are responsible for transporting heat energy, momentum, and chemical species, and so knowledge of the winds is crucial for understanding the temperature and compositional distribution in the upper atmosphere.

Unfortunately, there have been no Mars thermospheric wind measurements, and so our knowledge of thermospheric winds comes from model predictions. In a series of papers, Bougher et al. [1,2] described a temperature and wind climatology simulated by their Mars thermospheric general circulation model (MTGCM) for different portions of the solar cycle. Crowley et al. [3–6] developed a new first-principles model of the middle- and upper-atmosphere dynamics, energetics, and chemistry of Mars.

In this paper, we describe a new technique to derive neutral wind parameters from spacecraft accelerometer and rate gyro data in the 95–160-km region. In principle, both winds and densities can be derived from the Mars Global Surveyor (MGS) and Mars Odyssey missions. Some initial results will be placed in context by the use of the Crowley et al. [3–6] ASPEN model. Section II of the paper describes the MGS and Odyssey missions and the technique for obtaining cross-track winds. Both spacecraft are in 93-deg-inclination orbits, and so, except when they are very near the poles, the cross-track wind is essentially the zonal wind. Section III describes the ASPEN model. Section IV describes our results.

II. MGS and Odyssey Mission Overview

In this section, we describe the similarities and differences between the MGS and Odyssey spacecraft, aerobraking missions, and latitudinal–seasonal–diurnal coverage during the aerobraking phase. These two missions had significantly different latitudinal–seasonal profiles and different accelerometers and rate gyros, and they experienced significantly different atmospheric conditions.

A. Mars Global Surveyor Mission, Accelerometers, and Rate Gyros

MGS began aerobraking at Mars in 1997 (Esposito et al. [7,8]), with an orbital period of about 45 h. There were two interruptions in aerobraking during the mission. The first was from orbit 19 to orbit 40, due to the broken solar array (discussed later). Subsequently, a six-month hiatus occurred from orbit 202 to orbit 573. Aerobraking ended in February 1999 on orbit 1283, with the orbital period below 2 h and with an orbit inclination of about 93 deg.

MGS had integrating accelerometers [9], with a quantization sensitivity of 0.332 mm/s at a sample rate of 10/s. At each sample, the remainder was carried over to the next count so that sensitivity could be traded with temporal resolution. For a 1-s count time, atmospheric density was recovered to between 0.6 and 1 kg/km^3. During the aerobraking phase, MGS demonstrated the importance of dynamics in the thermosphere. MGS aerobraking around orbit 50 revealed a rapid response of the northern polar region to the Noachis regional dust storm in the southern hemisphere (45° S). Density increased by over a factor of 2 in a couple of days at 45° N, followed by a relaxation back to the nominal atmosphere over 50 to 100 days [9].

MGS had very accurate rate gyros driven by Mission Operations Center requirements for pointing knowledge and control. The gyros

Presented as Paper 6392 at the AIAA/AAS Astrodynamics Specialist Conference and Exhibit, Keystone, CO, 21–24 August 2006; received 30 October 2006; revision received 3 May 2007; accepted for publication 10 May 2007.

*President, Chief Scientist, 11118 Quail Pass; gcrowley@astraspace.net.
†Langley Professor.

had a quantization level of 1 μrad/s, which maps into detecting spacecraft heading changes of about 3 mrad for timescales of interest here. Such sensitivity would be theoretically capable of determining cross-track winds to 15 m/s. In Sec. III, we describe a technique to derive cross-track winds from accelerometer and rate gyro data throughout an aerobraking pass.

On orbit 15, there was an unexpected doubling of the atmospheric density at periapsis and a very large deflection of the solar array. The same solar array was known to have been damaged just after launch during deployment. Aerobraking was delayed while the problem was being studied and was not continued until orbit 40. Because of the broken array, the rate of aerobraking was limited to about one-half of the original design rate. To arrive at the required science orbit with the slower aerobraking rate, an "aerobraking hiatus" was built into the mission from orbit 201 until orbit 573. Aerobraking was then continued, with only one minor problem through orbit 1283. When excited by sudden changes in atmospheric density or large attitude-thruster firings, the solar array vibrated with a period of between 6 and 7 s. During these vibration periods, the quality of the data might be significantly reduced. However, by time-averaging or filtering the data, studies to determine properties of the atmosphere are possible, though with reduced spatial resolution.

B. Mars Odyssey Mission, Accelerometers, and Rate Gyros

Odyssey began aerobraking in October 2001, with an orbital period of about 18 h, and ended 300 orbits later in January 2002, with an orbital period of about 2 h. Odyssey also had an orbital inclination of about 93 deg. There were no mission or spacecraft anomalies that significantly affected the spatial coverage. The Odyssey accelerometers [10] had two internal counting and digitization systems so that the noise on the accelerometer data appeared essentially random. The raw data were at 200 Hz and quantized internally at 2.3 mm/s. The least significant bit in the output A/D converter was 0.0758 mm/s. For density recovery, the data were averaged over 1 s and the initial rms noise level for the 1-s data was about 0.09 mm/s. Because of onboard data storage limitations, the number of samples included to perform the 1-s average was reduced to 50 (orbit 138) and then to 20 (orbit 262), with consequential increases in noise.

Odyssey rate gyros had a rms random noise level about five times the MGS gyros' quantization. When mapped into heading and the ability to determine crosswinds, Odyssey data could produce crosswinds to 40-m/s accuracy. Both the accelerometer and gyro methods measure the rotation of the orbital velocity in the body frame. The orbital velocity is about 4000 m/s, and so the 40 m/s is based on a 1% measurement. Accelerometer noise is on the order of 0.04 mm/s and total acceleration during a typical aerobraking pass is about 20 mm/s, and so based on noise only, the anticipated angular noise would be about 0.1%. However, there are other error sources, most of which are not random (e.g., center-of-mass location affects gyro recovery, aerodatabase error, accelerometer bias, gyro drift, etc.). So the 40 m/s is based on inspection of typical recovered wind results, rather than a strict covariance analysis. Errors in the along-track position, velocity, and acceleration are negligible. Major improvements in future missions would include a perfectly symmetrical spacecraft. Even small asymmetries such as the high-gain antenna on Odyssey produce problems in the calculation of aerodynamic moments.

C. Comparison of Mars Global Surveyor and Mars Odyssey Spatial and Temporal Coverage

The spatial and temporal coverage for the two missions are illustrated in Fig. 1. The points correspond to the conditions at periapsis of each orbit. Aerobraking actually occurs along the orbital track for distances on both sides of periapsis, from 500 km early in the missions to 1200 km near the end of aerobraking. Both missions began aerobraking in the mid to high northern latitudes (Fig. 1d) during the northern hemisphere fall/winter period, with $180 < L_s < 360$. Initially, orbital precession carried the periapsis of both missions toward the North Pole. During the 370-orbit aerobraking hiatus, the MGS periapsis precessed over the pole and back to around 60° N latitude. Thus, except for the north polar cap, MGS provided pole-to-pole coverage, being at the southern pole near southern winter ($L_s = 90$). Except near the end of MGS aerobraking, atmospheric passage occurs in the afternoon (Fig. 1b) between 12–18 local time (LT). During the last 200 orbits, the local solar time (LST) moves from midafternoon to early morning. Data during these orbits should provide a comparison of winds and densities in the day and night and at approximately the same latitude. On the other hand, almost all aerobraking for Odyssey occurs at night (Fig. 1b) between 18–03 LT. Because of the broken solar array, MGS generally did not penetrate as deeply into the atmosphere as did Odyssey (Fig. 1c). As MGS approached the colder, lower-density, South Pole region, the aerobraking altitude was reduced to 100 km for a few orbits. Odyssey got to 95-km altitudes for a number of orbits while aerobraking inside the "polar vortex" region, and these passes are the focus of this paper.

D. Recovering Winds from Aerobraking Data

The use of accelerometer data to derive atmospheric densities is well-known. Tolson et al. [9–11] used the MGS and Odyssey in-track accelerometer data to derive atmospheric densities during aerobraking. Less well known is that a component of the neutral

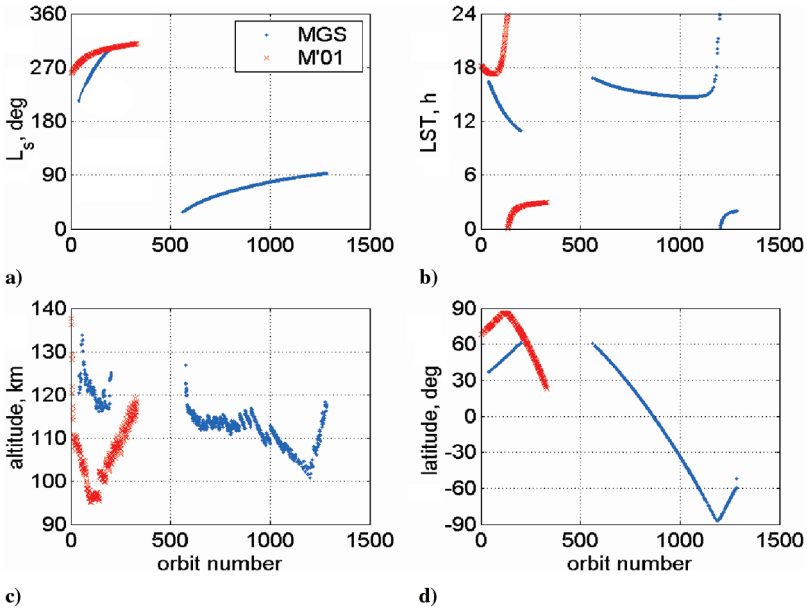

Fig. 1 Orbital synopsis for MGS (blue) and Odyssey M'01 (red) as a function of the orbit number; M'01 refers to Mars Odyssey 2001.

winds can be derived from the cross-track accelerations and rate gyro data.

A new technique for recovering crosswinds from gyro and accelerometer data is described here. For aerobraking operations, spacecraft are designed to have static aerodynamic stability. This means that there is an orientation specified by the pitch angle α and the yaw angle β relative to the wind that provides no net aerodynamic torque, called the *trim orientation*. As the spacecraft passes through the atmosphere, the aerodynamic torques tend to rotate the vehicle toward the trim orientation. A wind component orthogonal to the velocity will cause a change in the heading in inertial space, because the aerodynamic torques tend to align the vehicle to the trim orientation relative to the wind. A crosswind normal to the velocity that is horizontal (vertical) will cause the spacecraft to yaw (pitch) in inertial space. Changes in inertial trim directions can thus be related to relative crosswinds with a 100-m/s crosswind producing about a 1.4-deg change in heading.

If the vehicle did not deviate from the trim orientation due to phenomena other than winds, it would be a simple matter to determine the crosswind. However, during the initial phases of an aerobraking pass, the vehicle is seldom in the trim orientation. As aerodynamic torques begin to increase, the vehicle starts oscillating about the trim orientation. These oscillations are typically between 5 and 10 deg and tend to mask any change in orientation due to the winds. On some passes, the crosswind effects are clearly visible as a bias in the angle about which the vehicle is oscillating. To extract the most wind information from the data, one must resort to more extensive data analysis, as described later.

The development starts with the rotational equations of motion of a rigid body about the center of mass. The total angular momentum of the vehicle is given by

$$\boldsymbol{L} = \mathbf{I}\boldsymbol{\omega} + \mathbf{I}_{\mathrm{rw}}\boldsymbol{\omega}_{\mathrm{rw}} \tag{1}$$

where $\mathbf{I}$ is the moment of inertia of the vehicle, including the reaction wheels; $\boldsymbol{\omega}$ is the angular velocity of the vehicle measured by the gyros; $\mathbf{I}_{\mathrm{rw}}$ is the moment of inertia of the three reaction wheels; and $\boldsymbol{\omega}_{\mathrm{rw}}$ is the total angular velocity of the three wheels relative to the vehicle. Euler's equation for the rotational motion of the vehicle is

$$\mathbf{I}\,\frac{\mathrm{d}}{\mathrm{d}t}\boldsymbol{\omega} + \mathbf{I}_{\mathrm{rw}}\,\frac{\mathrm{d}}{\mathrm{d}t}\boldsymbol{\omega}_{\mathrm{rw}} + \boldsymbol{\omega} \times \mathbf{L} = \mathbf{T} \tag{2}$$

where $\mathbf{T}$ is the external torque applied to the vehicle. Note that all terms on the left can be calculated from the physical properties of the vehicle, telemetry body angular rates, and telemetry reaction wheel speeds. So the aerodynamic torque can be directly determined during each aerobraking pass. Given the torque components and ancillary data such as atmospheric density and vehicle velocity, the aerodynamic-moments database can be used to determine α and β.

Only one subtlety remains: Recovery of α and β from aerodynamic torques is very sensitive to center-of-mass (CM) location. The CM changes because there is liquid fuel onboard the vehicle. The amount of fuel changes through the mission as attitude control jets are fired and as orbit correction maneuvers are made. Consequently, the CM must be determined with the winds. As the vehicle begins an aerobraking pass, small drag forces overcome surface tension in the tank, and the fuel settles toward the forward area of the tank. In the analysis, it is usually assumed that the CM is constant during a pass, but it must be modeled as varying slowly from pass to pass. Throughout the mission, we assume that a linear relation exists between the CM location and mass of fuel in the tank. Fuel usage is based on the thruster on-time telemetry data.

Pitch and yaw angles can also be determined from the accelerometer data, which provide the cross forces on the spacecraft. However, the signal-to-noise ratio is much lower than for the torque-determined angles. On the other hand, the force-derived angles are not dependent on the CM location. The strongest solution for the crosswinds is obtained when both torque and force data are combined over a number of orbits. We formulated the problem as a nonlinear minimum-variance estimator for crosswinds and center-of-mass location with a priori covariance on the estimated parameters and the data.

III. ASPEN–Mars Model

Thermospheric general circulation models (TGCMs) were developed for the Earth by the National Center for Atmospheric Research (NCAR) beginning in the early 1980s to study the global temperature, circulation, and chemical structure of the Earth's thermosphere and its response to solar and auroral activity. The NCAR models have been an important tool for studies of the Earth's thermosphere and ionosphere. For example, Crowley et al. [12,13] discovered an important structure in the high-latitude neutral density and composition [14–19]. The thermosphere–ionosphere–mesosphere–electrodynamics general circulation model (TIME-GCM) [20] is the latest version of the NCAR model for Earth, predicting winds, temperatures, major and minor composition, electron densities, and electrodynamic quantities globally from 30 to 500 km. Many aspects of the TIME-GCM have been extensively validated against satellite and ground-based data over the last 10 years (Roble et al. [21], Lu et al. [22], Yee et al. [23], and Meier et al. [24]), and the model has played an important role in understanding the characteristics of the upper atmosphere of Earth. The codes were initially developed at NCAR for a Cray supercomputer environment. The TIME-GCM code was ported to a Linux PC environment in which a model day can be simulated in about 6 h on a single 2-GHz PC. Faster turnaround can be achieved using a Beowulf system [25].

We recently used the dynamic core of the TIME-GCM and modified it for Mars [3–6]. The new Mars model is called the advanced space environment (ASPEN) model, and it simulates the Martian atmosphere from about 14 km to the exobase, including the ionosphere. The model typically uses a fixed geographic grid with a 5×5 deg horizontal resolution and a vertical resolution of a quarter-pressure-scale height, although we can use a 2×2 deg version. The model time step is typically 1 min. The model currently does not include a magnetic field specification or coupling with the solar wind.

ASPEN–Mars currently solves for the neutral, electron, and ion temperature profiles, as well as for the compositional profiles of CO_2, N_2, and $O_X = (O + O_3)$, coupled through major-species-diffusion equations. It also includes minor species with transport and appropriate photochemistry: O_2, Ar, $N(^4S)$, $NO_X = (NO + NO_2)$, H_2O, H_2, CH_4, CO, and $HO_x = (H + OH + HO_2)$. The model also includes appropriate ion chemistry. The ASPEN model differs considerably from the Mars atmosphere model developed by Bougher et al. [1,2,26], because the latter was developed from an NCAR model that did not include either the middle-atmosphere chemistry required for Earth or Mars or electrodynamic capabilities.

The inputs required by ASPEN include the solar flux at 59 key wavelengths (bands and lines) and tides propagating up from below the 14-km lower boundary. The solar flux is specified using various parameterizations described in detail by Roble [20,27,28], including the solar EUV flux model for aeronomic calculations (EUVAC) [29], in which the fluxes are parameterized by the solar $F_{10.7}$ flux. These parameterizations were developed to represent the solar flux impinging on the Earth's atmosphere, but they should also be relevant to Mars, with a correction for heliospheric distance. Ionization and absorption cross sections are also required to compute the corresponding ionization and absorption rates for each wavelength. The development of the ASPEN model included the introduction of CO_2 chemistry and the appropriate cross sections to compute realistic ionization and temperature structures. A gravity-wave drag parameterization specifies the momentum deposition, heating, and turbulent mixing associated with gravity waves interacting with the general circulation. For the Earth, the gravity-wave parameterization is important because it allows the model to simulate both the mean circulation and tides in the upper mesosphere for equinox and solstice conditions [20]. The temperatures of the ASPEN lower boundary are specified using a simple seasonal climatology that we derived from MGS radio occultation measurements of temperature. They also agree reasonably well with the NASA Ames Research Center's model temperatures [30].

We compared the thermospheric structure in our ASPEN Mars model for equinox and solstice conditions with the Bougher et al.

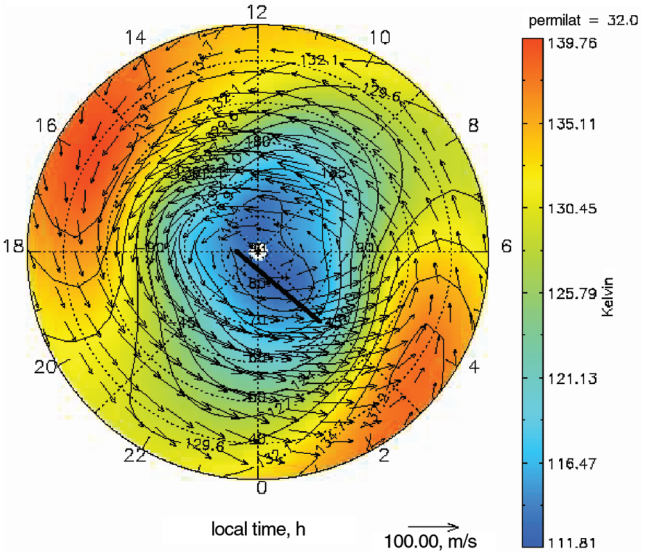

Fig. 2 Temperature for $L_s = 270$, 100 km, and perimeter latitude (permilat) of 32°.

[1,2] MTGCM results and found that the two models produce very similar results. ASPEN also predicts a solar cycle variation of thermospheric temperature structure that closely resembles that of the MTGCM [3–6]. We also validated the ASPEN model against measurements of the Mars atmosphere. For example, we compared against thermospheric densities from MGS accelerometer data, ionospheric electron densities from the MGS radio science instrument, and middle-atmosphere temperature profiles from the Spirit and Opportunity Rover descents [30–32].

IV. Results

We made preliminary comparisons of densities and winds for 10 orbits spread through the Odyssey mission. Figures 2–4 depict the results of one such validation study. Figure 2 shows the ASPEN global distribution of Mars' winds and temperatures at 100-km altitude as functions of latitude and local time for $L_s = 270$ (northern winter solstice) moderate solar activity ($F_{10.7} = 150$) conditions at 00 hrs Universal Time. The temperature is coldest near the pole, and the model winds are mainly zonal eastward, concentrated in a jet near 60° latitude. This behavior is characteristic of the winter season and the polar vortex. It has a counterpart in the Earth's stratosphere [33]. The corresponding density structure from ASPEN is shown in Fig. 3 for the same vortex study. Superposed on Figs. 2 and 3 is a line

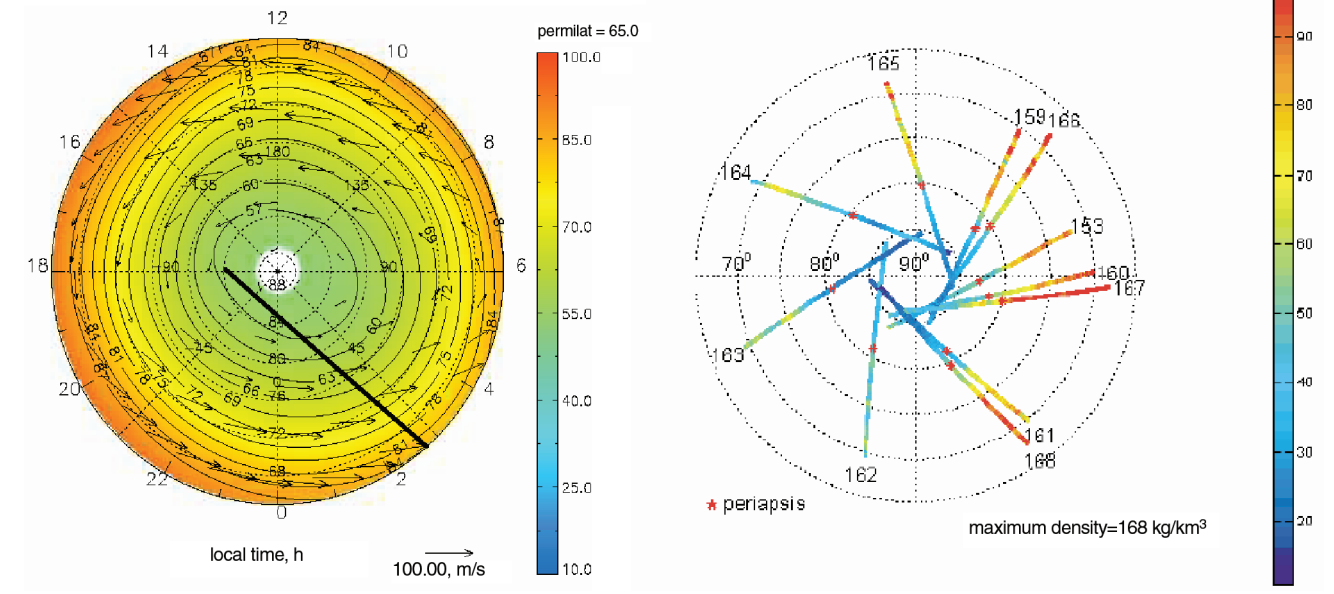

a) b)

Fig. 3 Density structure corresponding to the high-latitude portion of Fig. 2: a) ASPEN model with a perimeter latitude of 65° and b) Odyssey measurements with a perimeter latitude of 65°.

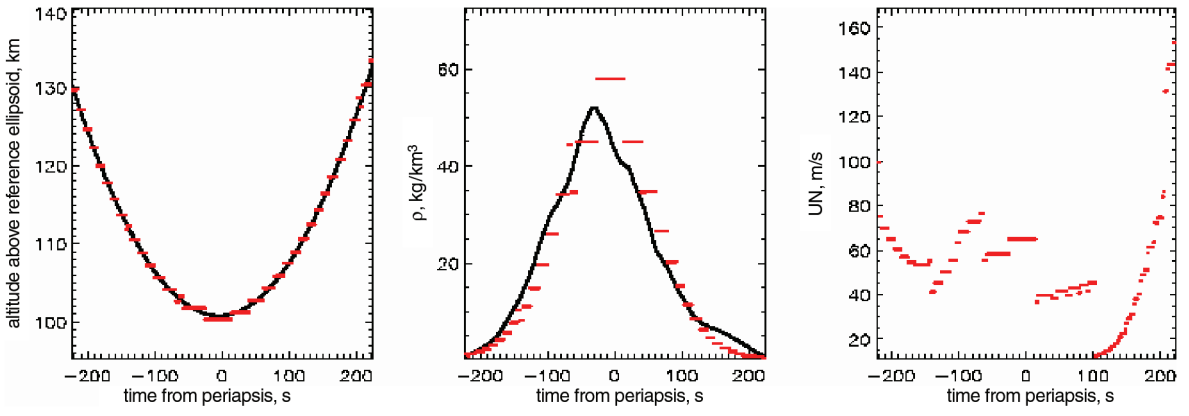

a) b) c)

Fig. 4 Comparison of ASPEN and Odyssey aerobraking results as functions of the time from periapsis: a) altitude, b) density, and c) zonal wind (UN) from ASPEN only.

showing one of the Mars Odyssey aerobraking passes (orbit 170) near solstice extending over the pole.

Figure 3b summarizes the densities obtained from orbits 153 and 159–168, mapped to a reference altitude of 100 km. Red stars indicate the location of periapsis. These results were obtained for aerobraking operations using a crude method for mapping density profiles to a reference altitude. The Odyssey data reveal a decreased density near the pole that is reminiscent of the density structure predicted by ASPEN. The ASPEN results suggest a weak wave 1 and 2 density variation, whereas the data suggest a strong wave-1 variation. However, care should be exercised when using the data results (in particular, density gradients) for quantitative analysis. Density estimates become less reliable away from periapsis, due to the crude mapping method used during operations.

Returning to the densities deduced from the onboard accelerometer on Odyssey, corresponding to Fig. 3, thermospheric densities are plotted in Fig. 4b as a function of time relative to periapsis. The altitude of the satellite (Fig. 4a) ranged from about 130 to 95 km during this pass and accounts for most of the density variation in Fig. 4b. Superposed on the satellite density data are densities extracted from the ASPEN GCM (red dashes).

Figures 2 and 3 suggested that a pass through the vortex at a fixed height of 100 km could experience cross-track winds of over 100 m/s in the same direction at the beginning and end of the pass, with nearly no crosswinds near the center of the pass. In fact, the ASPEN model reveals that the vortex structure changes with altitude, and the wind speeds have increased to 250 m/s at 160-km altitudes, as will be discussed in more detail later. Figure 4c depicts the zonal wind speed as a function of time from periapsis, as predicted by the model (note that we did not interpolate horizontally and vertically for this study, but simply used the closest model grid point). Also, the upward-propagating tides in the model were not tuned for the Odyssey conditions. The corresponding Odyssey data for orbit 170 are plotted in Fig. 5b. The red line is the altitude above the reference ellipsoid. The wind data show a 200-m/s jet with a width of about 200 s (∼13° downtrack), whereas the model (see Fig. 4c) shows a

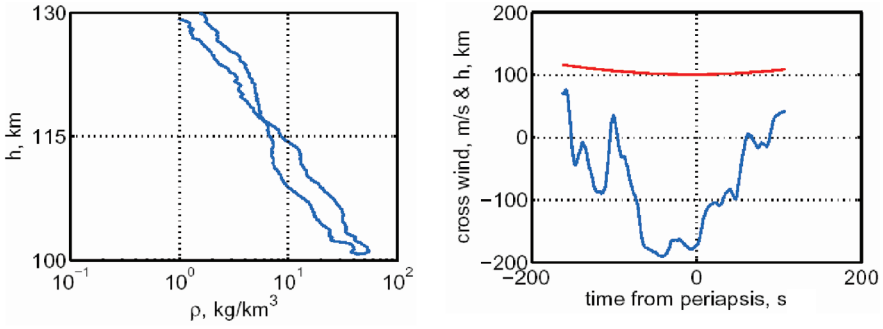

a) b)

Fig. 5 Odyssey altitude, density, and cross-track wind as functions of the time from periapsis.

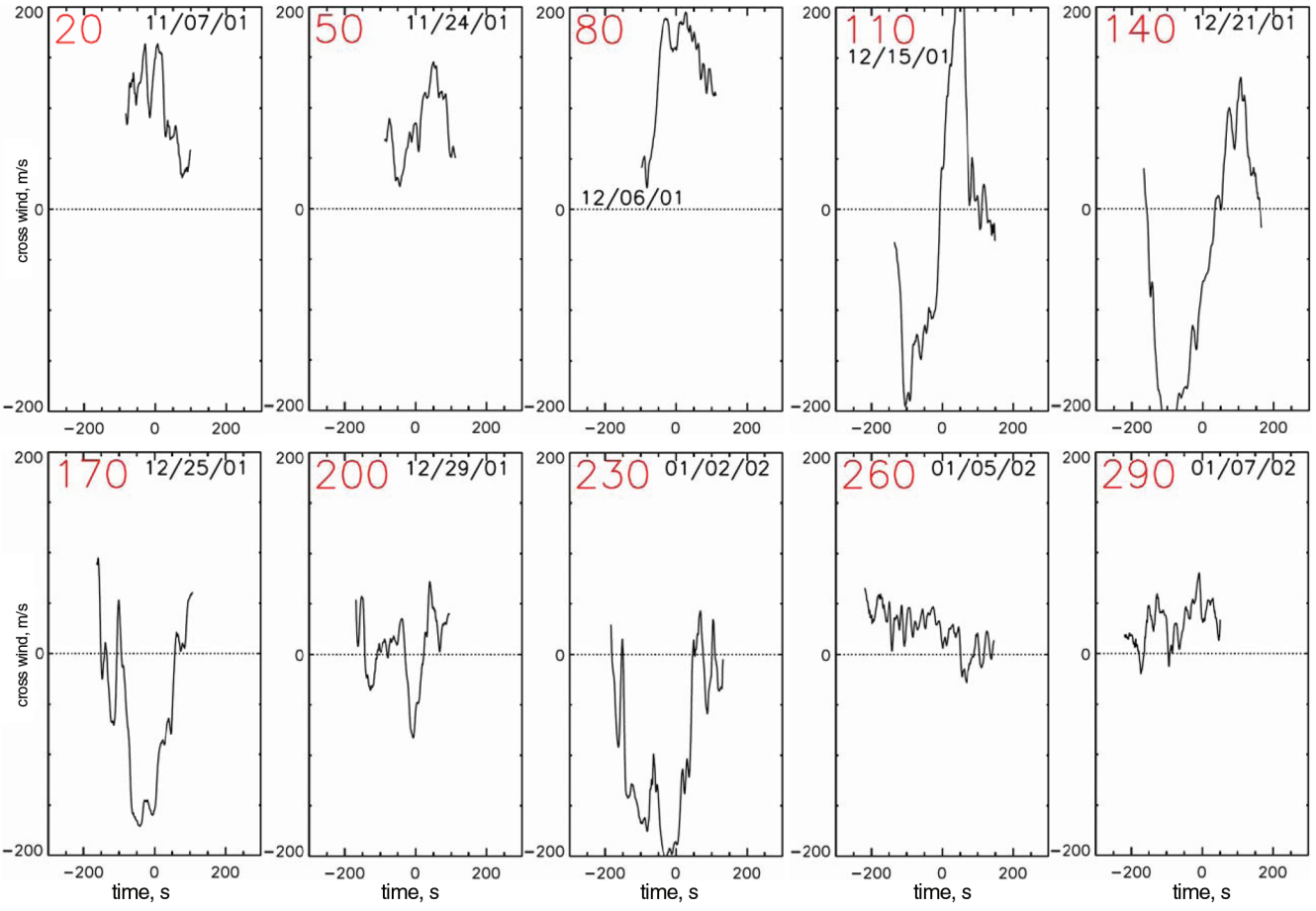

Fig. 6 Cross-track winds for 10 Odyssey aerobraking passes as functions of time in seconds from periapsis; pass numbers are in red, with corresponding dates.

somewhat broader and shallower jet of about 160 m/s. The difference in latitude of the center of the jet is difficult to quantify, but appears to be about 10°. The difference in relative magnitude could be due to a center-of-mass location error of less than 1 cm, which would bias the entire curve by about 250 m/s.

Figure 6 shows the results for all ten Odyssey orbits considered here. It is apparent that orbits 20–50 and 260–290 contained variations less than about 100 m/s, whereas orbits 80–230 contained variations greater than 100 m/s. These ten orbits spanned the date range of 7 November 2001 to 7 January 2002, a period of two months. During that time, the location of periapsis moved from the day side at 70° N and 17.8 LT over the North Pole to the night side at 42° N and 2.8 LT. (The latitude and local time of periapsis for each orbit are listed in Fig. 7.) The smaller wind variations observed in Fig. 6 tend to be at the lower latitudes: less than 80° N on the day side and less than 55° N on the night side. We suggest that these smaller winds are caused by the spacecraft sampling outside the main vortex. We also examined the $F_{10.7}$ index at Earth (not Mars) during the three-month period near solar maximum during the dates of the Odyssey orbits. The relative location of Mars at this time means that it would have experienced these fluxes about six days before the Earth observations. There does not appear to be any correlation between wind shear and $F_{10.7}$ corrected to Mars.

MGS and Odyssey experienced rapidly changing conditions along the aerobraking track, with large wind shears, and therefore a simple interpretation of the MGS and Odyssey winds is not possible. Instead, a model such as ASPEN is required, to provide a framework for interpretation of the variations in the wind and density data. In a future paper, we will provide a detailed comparison of each of the Odyssey orbits, with the corresponding model prediction. For the moment, we provide Fig. 7, which shows the neutral wind speed and direction as functions of altitude between 95–140 km from ASPEN at the location of periapsis in each panel of Fig. 6. The blue circle represents the wind at 95 km, and each red dot represents an altitude increase of 5 km. The model results depict wind shears up to 150 m/s over the 95–140-km range, but the figure suggests that the largest wind shears in the model were present for the earlier day-side orbits and generally grew smaller as the months progressed and periapsis moved to the night side and lower latitudes. Further analysis of the model results is required to clarify why the wind shears behaved in this fashion and how they are related to the location of the polar vortex contained in the model.

V. Conclusions

We described a new technique for the retrieval of cross-track winds from satellite accelerometer and rate gyro data in the 95–160-km region. We applied the technique to a subset of data from the Mars Global Surveyor and Odyssey missions, and 10 Odyssey aerobraking passes were studied here. The cross-track winds are mainly zonal, and the data suggest that large wind shears occurred between 160–100 km, and changes of 100–200 m/s appear common. There are many questions that need to be addressed concerning the validity of the wind retrievals from MGS and Odyssey. The ASPEN first-principles model of the Martian atmosphere predicts large wind shears in the 160–100-km region, comparable with those estimated from the Odyssey data, and appears to confirm that the initial wind results are reasonable. Further analysis will permit us to answer key science questions regarding thermospheric winds on Mars using the MGS and Odyssey data.

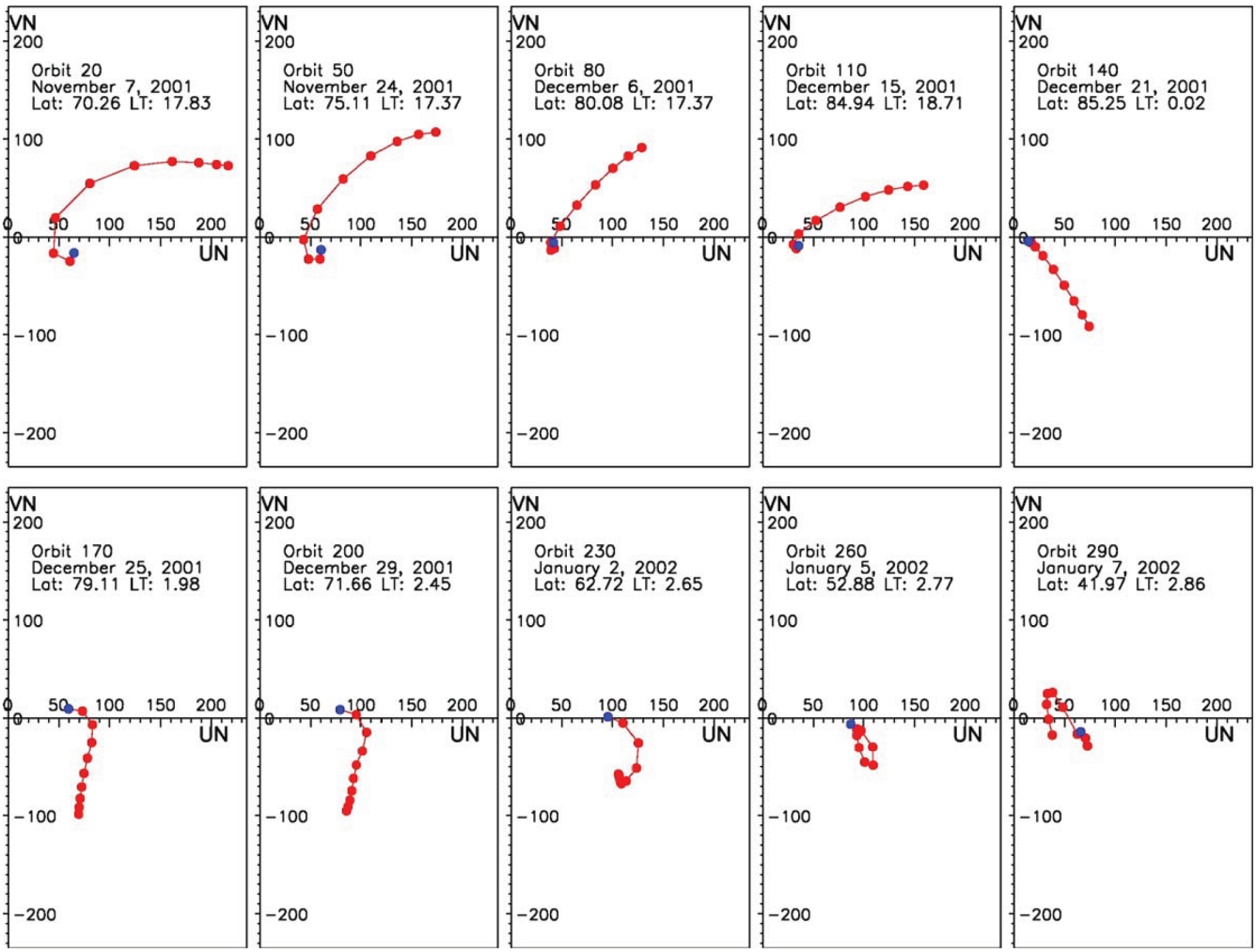

Fig. 7 Wind vector [components: zonal wind (UN) and meridional wind (VN)] from 95–140 km at 5-km intervals from ASPEN model simulations corresponding to 10 Odyssey aerobraking passes between 7 November 2001 and 7 January 2002; the blue dot represents 95 km.

Acknowledgment

The authors acknowledge the participation of Darren Baird in the development of the technique described here.

References

[1] Bougher, S. W., Engel, S., Roble, R. G., and Foster, B., "Comparative Terrestrial Planet Thermospheres, 2: Solar Cycle Variation of Global Structure and Winds at Equinox," *Journal of Geophysical Research*, Vol. 104, No. E7, 1999, pp. 16,591–16,611.

[2] Bougher, S. W., Engel, S., Roble, R. G., and Foster, B., "Comparative Terrestrial Planet Thermospheres, 3: Solar Cycle Variation of Global Structure and Winds at Solstices," *Journal of Geophysical Research*, Vol. 105, No. E7, 2000, pp. 17,669–17,692.

[3] Crowley, G., Bullock, M. A., Freitas, C. J., Boice, D. C., Young, L. A., Grinspoon, D. H., Gladstone, R., Link, R., and Huebner, W. F., "2002 Development of a New Mars Atmosphere Model," *Bulletin of the American Astronomical Society*, Vol. 34, Abstract 15.18, 2002, p. 865.

[4] Crowley, G., Bullock, M. A., Freitas, C., Chocron, S., Hackert, C., Boice, D., Young, L., Grinspoon, D. H., Gladstone, R., Huebner, W., Wene, G., and Westerhoff, M., "Development of a Surface-to-Exosphere Mars Atmosphere Model," *Sixth International Mars Conference* [CD-ROM], NASA Goddard Space Flight Center, Greenbelt, MD, and Jet Propulsion Lab, California Inst. of Technology, Pasadena, CA, July 2003.

[5] Crowley, G., Bullock, M. A., Freitas, C., Boice, D., Young, L., Chocron, S., Hackert, C., Wene, G., Westerhoff, M., Gladstone, R., Link, R., Grinspoon, D. H., and Huebner, W., "Development of a Surface-to-Exosphere Mars Atmosphere Model" [online abstract], Mars Atmosphere Modelling and Observations Workshop, Granada, Spain, available at http://www-mars.lmd.jussieu.fr/granada2003/abstract/crowley.pdf, Jan. 2003.

[6] Crowley, G., Bullock, M. A., Freitas, C. J., Chocron, S., Hackert, C., Boice, D., Young, L. A., Grinspoon, D. H., Gladstone, G. R., Huebner, W., Wene, G., and Westerhoff, M., "A New Surface to Exosphere Mars Atmosphere Model," *Bulletin of the American Astronomical Society*, Vol. 35, Abstract 14.05, 2003, p. 934.

[7] Esposito, P., Johnston, M., Graat, E., and Alwar, V., "Navigation and the Mars Global Surveyor Mission," *Proceedings of the 12th International Symposium on Space Flight Dynamics*, ESA SP-403, ESA, Paris, Aug. 1997, pp. 371–376.

[8] Esposito, P., Alwar, V., Demcak, S., Graat, E., Johnston, M., and Mase, R., "Mars Global Surveyor Navigation and Aerobraking at Mars," American Astronautical Society Paper 98-384, 1998; also available at http://marsprogram.jpl.nasa.gov/mgs/sci/aerobrake/SFD/SFD-Paper.html.

[9] Tolson, R. H., Keating, G. M., Cancro, G. J., Parker, J. S., Noll, S. N., and Wilkerson, B. L., "Application of Accelerometer Data to Mars Global Surveyor Aerobraking Operations," *Journal of Spacecraft and Rockets*, Vol. 36, No. 3, May–June 1999, pp. 323–329.

[10] Tolson, R. H., Keating, G. M., Dwyer, A., Hanna, J., George, B., Escalera, P., and Werner, M., "Applications of Accelerometer Data to Mars Odyssey Aerobraking and Atmospheric Modeling," *Journal of Spacecraft and Rockets*, Vol. 42, No. 3, 2005, pp. 435–443.

[11] Tolson, R. H., Keating, G. M., Noll, S. N., Baird, D. T., and Shellenberg, T. J., "Utilization of Mars Global Surveyor Accelerometer Data for Atmospheric Modeling," *Astrodynamics 1999*, Advances in the Astronautical Sciences, Vol. 103, American Astronautical Society, San Diego, CA, 2000, pp. 1329–1346.

[12] Crowley, G., Emery, B. A., Roble, R. G., Carlson, H. C., and Knipp, D. J., "Thermospheric Dynamics During the Equinox Transition Study, 1: Model Simulations for Sept. 18 and 19, 1984," *Journal of Geophysical Research*, Vol. 94, No. A12, 1989, pp. 16,925–16,944.

[13] Crowley, G., Emery, B. A., Roble, R. G., Carlson, H. C., Salah, J. E., Wickwar, V. B., Miller, K. L., Oliver, W. L., Burnside, R. G., and Marcos, F. A., "Thermospheric Dynamics During the Equinox Transition Study of September 1994, 2: Validation of the NCAR-TGCM," *Journal of Geophysical Research*, Vol. 94, No. A12, 1989, pp. 16,945–16,960.

[14] Crowley, G., Schoendorf, J., Roble, R. G., and Marcos, F. A., "Satellite Observations of Neutral Density Cells in the Lower Thermosphere at High Latitudes," *The Upper Mesosphere and Lower Thermosphere: A Review of Experiment and Theory*, Geophysical Monograph No. 87, American Geophysical Union, Washington, DC, 1995, pp. 339–348.

[15] Crowley, G., Schoendorf, J., Roble, R. G., and Marcos, F. A., "Cellular Structures in the High Latitude Lower Thermosphere," *Journal of Geophysical Research*, Vol. 101, No. A1, 1996, pp. 211–223.

[16] Crowley, G., Schoendorf, J., Roble, R. G., and Marcos, F. A., "Neutral Density Cells in the Lower Thermosphere at High Latitudes," *Advances in Space Research*, Vol. 18, No. 3, 1996, pp. 69–74.

[17] Schoendorf, J., and Crowley, G., "Interpretation of an Unusual High Latitude Density Decrease in Terms of Thermospheric Density Cells," *Geophysical Research Letters*, Vol. 22, No. 22, 1995, pp. 3023–3026.

[18] Schoendorf, J., Crowley, G., Roble, R. G., and Marcos, F. A., "Neutral Density Cells in the High Latitude Thermosphere: Morphology for Solar Maximum Deduced from TIGCM Simulations," *Journal of Atmospheric and Terrestrial Physics*, Vol. 58, No. 15, 1996, pp. 1751–1768.

[19] Schoendorf, J., Crowley, G., and Roble, R. G., "Formation Mechanism for Thermospheric Neutral Density Cells at High Latitudes," *Journal of Atmospheric and Terrestrial Physics*, Vol. 58, No. 15, 1996, pp. 1769–1781.

[20] Roble, R. G., and Ridley, E. C., "Thermosphere-Ionosphere-Mesosphere-Electro Dynamics General Circulation Model (TIME-GCM): Equinox Solar Cycle Minimum Simulations (300–500 km)," *Geophysical Research Letters*, Vol. 22, No. 6, 1994, pp. 417–420.

[21] Roble, R. G., Killeen, T. L., Spencer, N. W., Heelis, R. A., Reiff, P. H., and Winningham, J. D., "Thermospheric Dynamics During November 21–22, 1981: Dynamics Explorer Measurements and Thermospheric General Circulation Model Predictions," *Journal of Geophysical Research*, Vol. 93, No. A1, 1988, pp. 209–225.

[22] Lu, G., Pi, X., Richmond, A. D., and Roble, R. G., "Variations of Total Electron Content During Geomagnetic Disturbances: A Model/Observation Comparison," *Geophysical Research Letters*, Vol. 25, No. 3, 1998, pp. 253–256.

[23] Yee, J. H., Crowley, G., Roble, R. G., Skinner, W., and Hays, P. B., "Global simulation of $O(^1S)$, $O_2(^1S)$ and OH Mesospheric Nightglow Emissions," *Journal of Geophysical Research*, Vol. 102, No. A9, 1997, pp. 19,949–19,968.

[24] Meier, R. R., Crowley, G., Strickland, D. J., Christensen, A. B., Paxton, L. J., Morrison, D., and Hackert, C. L., "First Look at the 20 November 2003 Superstorm with TIMED/GUVI: Comparisons with a Thermospheric Glocal Circulation Model," *Journal of Geophysical Research*, Vol. 110, 2005, Paper A09S41.

[25] Crowley, G., Freitas, C., Ridley, A., Winningham, D., Roble, R. G., and Richmond, A. D., "Next Generation Space Weather Specification and Forecasting Model," *Proceedings of the Ionospheric Effects Symposium*, edited by J. M. Goodman, JMG Associates, Alexandria, VA, under sponsorship from U.S. Naval Research Lab., Washington, DC, Oct. 1999, pp. 34–41.

[26] Bougher, S. W., Fesen, C. G., Ridley, E. C., and Zurek, R. W., "Mars Mesosphere and Thermosphere Coupling: Semidiurnal Tides," *Journal of Geophysical Research*, Vol. 98, No. E2, 1993, pp. 3281–3295.

[27] Roble, R. G., "Energetics of the Mesosphere and Thermosphere," *The Upper Mesosphere and Lower Thermosphere: A Review of Experiment and Theory*, edited by R. M. Johnson and T. L Killeen, Geophysical Monograph No. 87, American Geophysical Union, Washington, DC, 1995, pp. 1–21.

[28] Roble, R. G., "On the Feasibility of Developing a Global Atmospheric Model Extending from the Ground to the Exosphere," *Atmospheric Science Across the Stratopause*, edited by D. E. Siskind, S. D. Eckerman, and M. E. Summers, Geophysical Monograph No. 123, American Geophysical Union, Washington, DC, 2000, pp. 53–67.

[29] Richards, P. G., Fennelly, J. A., and Torr, D. G., "EUVAC: A Solar EUV Flux Model for Aeronomical Calculations," *Journal of Geophysical Research*, Vol. 99, No. A7, 1994, pp. 8981–8992.

[30] Crowley, G., Curtis, N., Hackert, C., Hinson, D., Wene, G., Freitas, C., Chocron, S., Bullock, M., and Roble, R. G., "Modeling Space Weather Effects on the Middle and Upper Atmosphere of Mars," *Journal of Geophysical Research* (to be published).

[31] Curtis, N., Crowley, G., Hackert, C., Hinson, D., Wene, G., Freitas, C., Chocron, S., Bullock, M., Roble, R. G., Boice, D., Young, L. A., Grinspoon, D., and Huebner, W., "Modeling Space Weather Effects on the Middle and Upper Atmosphere of Mars," *EOS, Transactions, American Geophysical Union*, Vol. 85, No. 17, Joint Assembly Supplement, Abstract SA31A-01, May 2004.

[32] Curtis, N., Crowley, G., Hackert, C., Hinson, D., Wene, G., Freitas, C., Chocron, S., Bullock, M., and Roble, R. G., "Modeling the Middle and Upper Atmosphere of Mars for Late 2003 to Early 2004," *EOS, Transactions, American Geophysical Union*, Vol. 86, No. 18, Joint Assembly Supplement, Abstract P21F-02, 2005.

[33] Schoeberl, M. R., and Hartmann, D. L., "The Dynamics of the Stratospheric Polar Vortex and Its Relation to Springtime Ozone Depletions," *Science*, Vol. 251, 4 Jan. 1991, pp. 46–52.

A. Ketsdever
Associate Editor